Pulse Oximetry Using Organic Optoelectronics under Ambient Light

Donggeon Han,* Yasser Khan, Jonathan Ting, Juan Zhu, Craig Combe, Andrew Wadsworth, Iain McCulloch, and Ana C. Arias*

Light absorption in oxygenated and deoxygenated blood varies appreciably over the visible and near-infrared spectrum. Pulse oximeters use two distinct wavelengths of light to measure oxygen saturation SpO2 of blood. Currently, light-emitting diodes (LEDs) are used in oximeters, which need additional components to drive them and negatively impact the overall size of the sensor. In this work, an ambient light oximeter (ALO) is demonstrated, which can measure photoplethysmography signals and SpO2 using various kinds of ambient light, avoiding the use of LEDs. Spectral filters are combined with organic photodiodes to create the ALO with sensitivity peaks at green (525 nm), red (610 nm), and near-infrared (740 nm) wavelengths. Finally, the wearable ALO is used to measure photoplethysmography signals and SpO2 on the index finger in different indoor and outdoor lighting conditions and the measurements are validated with commercial pulse oximeters under normal and ischemic conditions.

1. Introduction

Photoplethysmography (PPG) is a noninvasive optical technique for detecting blood volume changes, which uses a light source and a detector placed on the skin.[1] With each heartbeat, the blood volume in the arteries changes, consequently, altering the light attenuation through blood and tissue. PPG sensors measure this change in the optical signal using organic or inorganic light-emitting diodes (LEDs) and photodiodes (PDs). PPG can provide critical information about human health by providing vital signs (heart rate and blood pressure), vascular conditions, and cardiovascular

Dr. D. Han, Dr. Y. Khan, J. Ting, Dr. J. Zhu, Prof. A. C. Arais
Department of Electrical Engineering and Computer Sciences
University of California
Berkeley, CA 94720, USA
E-mail: groovyauro@gmail.com; acarias@eecs.berkeley.edu
Dr. C. Combe, Prof. I. McCulloch
Physical Science and Engineering Division
King Abdullah University of Science and Technology
Thuwal 23955-6900, Saudi Arabia
Dr. A. Wadsworth
Department of Chemistry
Imperial College London
London SW72AZ, UK

The ORCID identification number(s) for the author(s) of this article can be found under https://doi.org/10.1002/admt.201901122.

variability.[2] When PPG signals are obtained from two specific portions of the light spectrum, oxygen saturation SpO2 can be estimated by taking a ratiometric measurement. This method takes advantage of the different light absorption characteristics of oxyhemoglobin HbO2 and deoxyhemoglobin Hb at the two light spectra. Pulse oximetry utilizes the aforementioned method to obtain SpO2 and is widely used clinically as it is a safe and accurate way of measuring SpO2 and heart rate.[2,3]

By design, pulse oximeters require LEDs and PDs that can operate at two different spectra. The two spectra can either be green and red or red and near-infrared (NIR), where the spectrum ranges are—470 nm < green < 550 nm, 620 nm < red < 690 nm, and 740 nm < NIR < 950 nm.[4] Preferably, the overlap between the two spectra should be minimized for better accuracy in SpO2 calculation. Usually, a PD that can sense a broad range of the spectrum is selected and combined with two LEDs which can provide two different incident light spectrum. Most oximeters have been designed using this two-LEDs and one-PD (2L1P) configuration.[2,3,5–9] With this scheme, the PD itself cannot distinguish the wavelength of the incident light. The two LEDs must operate sequentially at a given frequency and the PD is synced accordingly by the optoelectronics driving hardware and software. Moreover, the operation of LEDs requires additional components which contribute to the current bulky form factors of conventional pulse oximetry and need further effort to reduce the power consumption of the LEDs.[10,11]

Another design for pulse oximeters utilizes one-LED and two-PDs (1L2P) configuration, where the LED is a broadband light source and the two PDs are sensitive at the two different spectra of interest. The 1L2P concept of detecting changes in tissue oxygenation was previously demonstrated by Bansal et al.[12] A wide spectrum organic LED which had both red and NIR components and two organic photodiodes (OPDs) with filters to distinguish the two different spectra were used to construct the sensor. Although the two OPDs had nonnegligible spectral overlap that negatively influenced precise measurements at red and NIR wavelengths, a relative change in the tissue oxygenation was successfully measured. The 1L2P configuration can simplify pulse oximeter designs because

**ADVANCED
SCIENCE NEWS**
www.advancedsciencenews.com

**ADVANCED
MATERIALS
TECHNOLOGIES**
www.advmattechnol.de

precise timing and sequential LED operations are not required. Nonetheless, it still requires LED, which needs to be controlled by an LED driver, so there is not much advantage over 2L1P configuration.

Recently, a vast range of flexible and stretchable opto-electronic sensors have been reported for PPG, oximetry, and other wearable and implantable medical sensing applications.[4,6–9,13,14] The soft form factors of these devices provide conformal contact with the human body, which enhances the signal-to-noise ratio compared to rigid electronics. Additionally, these sensors can be easily integrated into garments or wearable accessories.[15–21] When these soft optoelectronic sensors mold to the skin, the quality of the acquired signal enhances significantly. The use of flexible OPDs for PPG measurement has been shown to reduce noise current from ambient light.[6] OPDs also demonstrate other advantages such as lightweight, reduced fabrication complexity, and mechanical flexibility.[22] The aforementioned characteristics make flexible OPDs an excellent choice for wearable PPG and oximetry.

One of the features that distinguish organic absorbers from others is that their spectral sensitivities are relatively narrow compared to their inorganic counterparts.[23] Silicon PDs are broadband and they require carefully designed rigid band-pass filters in order to have good spectral selectivity. Organic materials can be easily designed to be insensitive in the infrared region and have partial absorption in the visible spectrum. This means that they can inherently possess spectral cutoffs within or near the visible spectrum, which can be utilized to realize spectral selectivity.

Most of the reported pulse oximeters in the literature use different combinations of LEDs and PDs—2L1P or 1L2P. Here, we demonstrate an ambient light oximeter (ALO) which utilize ambient light as the light source, circumventing the requirement for LEDs, and use two spectrally selective OPDs (0L2P). Organic absorbers are chosen so that the fabricated OPDs will be able to sense green, red, and NIR light. Bulk heterojunction blends of poly[N-9″-hepta-decanyl-2,7-carbazole-alt-5,5-(4′,7′-di-2-thienyl-2′,1′,3′-benzothiadiazole)] (PCDTBT) with [6,6]-phenyl C70-butyric acid methyl ester (PCBM70) or poly(3-hexylthiophene) (P3HT) with ((5Z,5′Z)-5,5′-(((4,4,9,9-tetraoctyl-4,9-dihydro-s-indaceno[1,2-b:5,6-b′]-dithiophene-2,7-diyl)bis(benzo[c][1,2,5]thiadiazole-7,4-diyl))-bis(methanylylidene))bis(3-ethyl-2-thioxothiazolidin-4-one)) (O-IDTBR) are used. The OPDs are flexible and compatible with roll-to-roll printing techniques.[22] These are combined with appropriate flexible filters that allow the OPDs to become spectrally selective (SS-OPDs) and sense green, red, or NIR light with minimal spectral overlap. Using these SS-OPDs, we collected PPG signals from various ambient lights sources: i) sunlight, ii) fluorescent, iii) LED, and iv) incandescent lights. Moreover, two different SS-OPDs are used together to form the ALO and perform pulse oximetry under sunlight. Finally, we show that our ALO can accurately detect varying oxygen saturation levels in the body, where the concentration of the inhaled oxygen is controlled using an altitude simulator. We also demonstrate a wearable ALO system, where the sensor is integrated into a glove form factor with wireless data transmission capability.

2. Results and Discussion

2.1. Spectral Selective Green, Red, and NIR Organic Photodiodes

The fundamental building blocks of our oximeter are the SS-OPDs, which are composed of OPDs and spectral filters. **Figure 1**a shows the device structure of OPDs used in this work. Although the spectral sensitivities of the organic absorbers are relatively selective, the spectra of OPDs are usually not narrow enough to distinguish the color of the incident light. In order to make the spectral sensitivities of the OPDs narrower and to make sure there is minimal overlap among different spectral OPDs, the OPDs in Figure 1a are combined with commercially available spectral filters. The band diagram of the OPDs is shown in Figure 1b. This makes the OPDs sense distinctly different spectral regions, which makes them SS-OPDs. Figure 1c shows the schematic top view of the completed ALO. It consists of two SS-OPDs which are placed 2 mm apart where one of the SS-OPDs senses red light and the other one senses either green or NIR light. External quantum efficiencies (EQEs) of three SS-OPDs are given in Figure 1d, where green, red, and NIR light can be sensed, respectively. When two different sets of PPG signals are collected from two SS-OPDs, pulse oximetry can be performed. For pulse oximetry, any light source containing red and green or red and NIR can be utilized. For example, the Sun is a natural source of light that can provide an abundant amount of red, green and NIR light. The normalized spectrum of the four different light sources used in this work—sunlight, fluorescent, LED, and incandescent lights are shown in Figure 1e. All the light sources have contributions in the green and red spectrum, while only sunlight and incandescent lights have strong NIR contributions. For a system level implementation, we demonstrate the use of our ALO outdoors under sunlight in a wearable form factor (Figure 1f).

In order to achieve green, red, and NIR SS-OPDs (referred to as green, red, and NIR sensors in the future text), organic photoactive layers and filters are carefully paired by considering their optical characteristics as shown in **Figure 2**. PCDTBT:PCBM70 is chosen as the photoactive layer for green and red sensors because of its absorption in the green and red regions. It is also widely used for studies in organic solar cells or OPDs due to its stability and reproducibility.[22,24–29] Optical characteristics of filters that were considered are shown in Figure S1 in the Supporting Information. Figure 2a shows the optical characteristics of the photoactive layer and filters for the green and red sensors. Blade-coated PCDTBT:PCBM70 film absorbs most of the visible spectrum and demonstrates a decrease in absorbance starting from around 600 and to 700 nm. The absorbance is negligible in the NIR region. When this spectrum is combined with the transmittance of the green filter (Kodak 58, Optical Wratten Filter), only the green portion ranging from 490 to 570 nm with a peak at 525 nm will be absorbed. The NIR portion (>715 nm) of the filters transmittance will be eliminated since there is negligible absorbance of PCDTBT:PCBM70 in the NIR. The red filter (Kodak 25, Optical Wratten Filter) transmits light starting from 590 nm, all the way up to the NIR. When this filter is combined with PCDTBT:PCBM70, the red portion starting from 590 to 700 nm will be sensed, where the lower spectrum
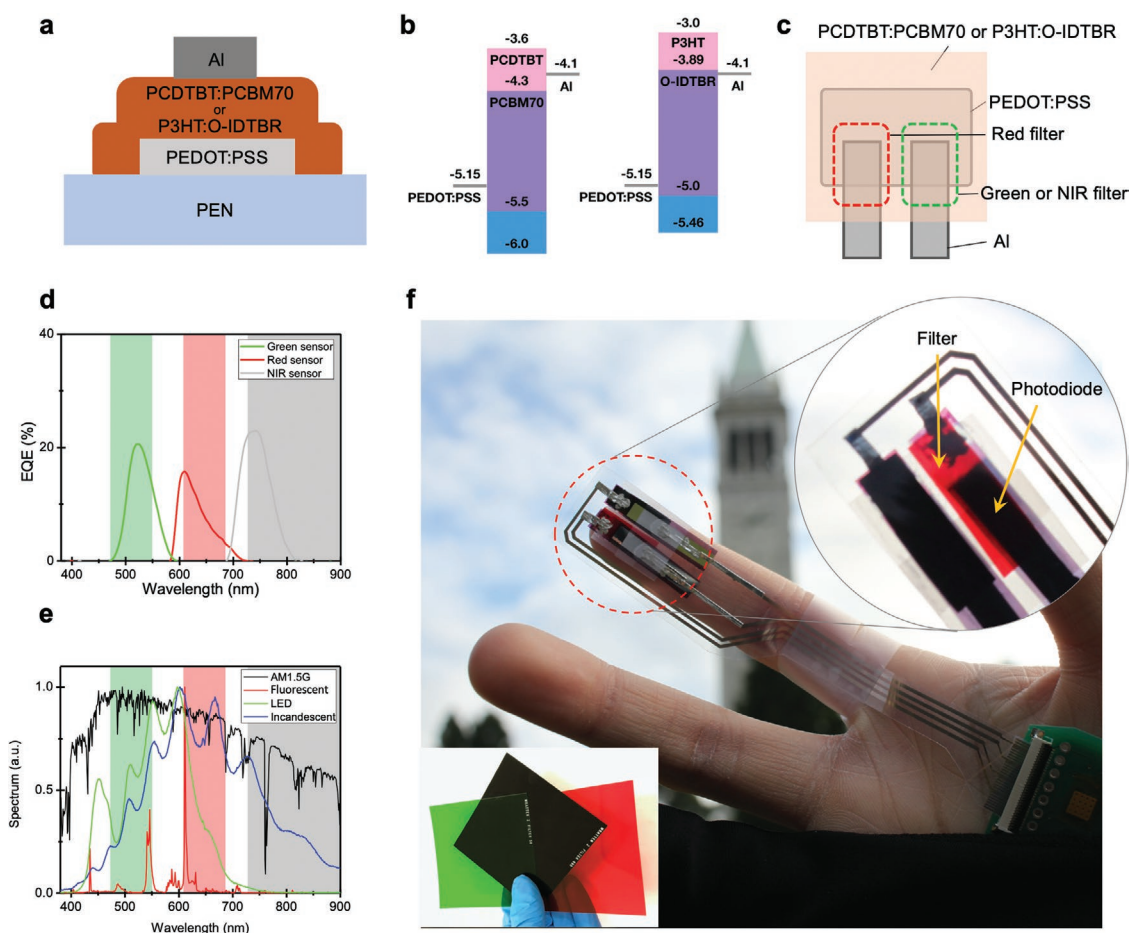
Figure 1. Photographs and schematics of the ambient light oximeter (ALO) composed of organic photodiodes with spectral filters, without any controlled light source. a) A schematic of the printed OPD structure. b) Band diagram of the OPDs used in this study. c) A schematic layout of the ALO. d) External quantum efficiencies of the green, red, and NIR sensors used in this work. The sensors are designed in such a way that there is negligible spectral overlap among the sensors. e) Normalized spectrum of AM1.5G sunlight, fluorescent, LED, and incandescent lights. All the light sources have contributions in the green and red regions of interest, while only sunlight and incandescent lights have strong NIR light. f) A photograph of the ALO worn on the index finger, which is connected to a wireless circuit board. The oximeter is composed of two printed organic photodiodes (OPDs) with spectral filters. Red, NIR, and green spectral filters are shown in the inset picture.

region is defined by the filter and the upper by the photoactive layer. For the NIR sensor, however, PCDTBT:PCBM70 cannot be used since it does not absorb in the NIR. P3HT:O-IDTBR

absorbs beyond the visible spectrum to the NIR.[30] Figure 2b shows the optical characteristics of the photoactive layer and filter for NIR sensor. Blade-coated P3HT:O-IDTBR film absorbs
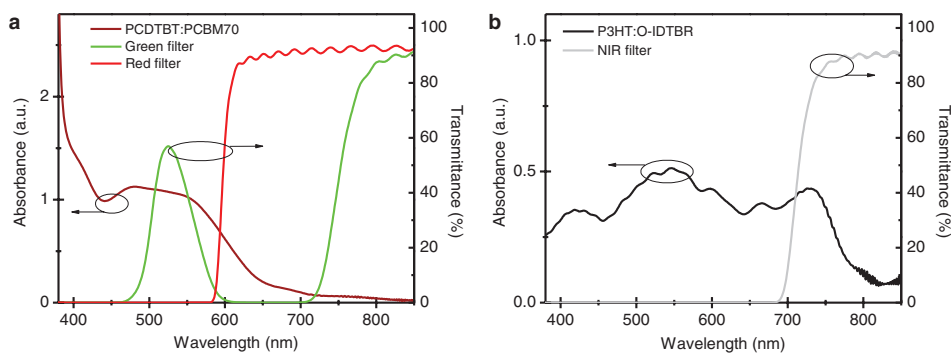

Figure 2. Optical characteristics of organic absorbers and spectral filters used to create green, red, and NIR sensors. a) Absorbance of blade-coated PCDTBT:PCBM70 film and transmittance of the green and red filters. The photoactive layer and filters are combined to make the green and red sensitive organic photodiodes. b) Absorbance of blade-coated P3HT:O-IDTBR and transmittance of the NIR filter. The photoactive layer and filter are combined to make the NIR sensitive organic photodiode.
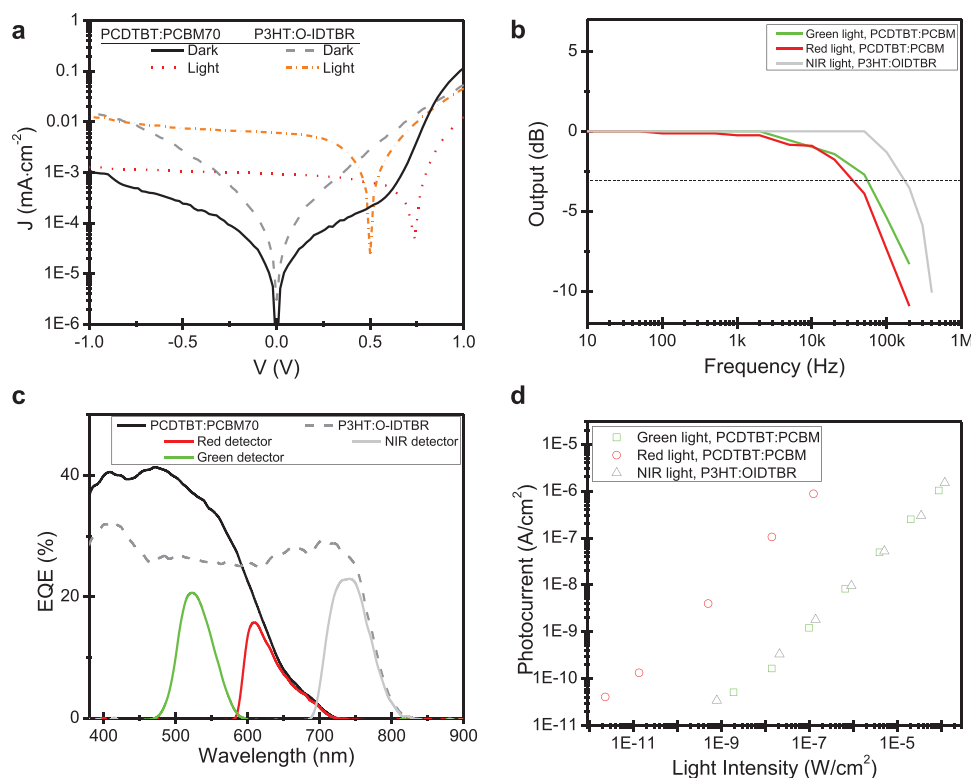
**ADVANCED
SCIENCE NEWS**

www.advancedsciencenews.com

**ADVANCED
MATERIALS
TECHNOLOGIES**

www.advmattechnol.de

Figure 3. Optical and electrical characteristics of the spectral selective OPDs. a) Current density (J)–voltage (V) characteristics of OPDs based on PCDTBT:PCBM70 or P3HT:O-IDTBR under dark or light conditions. Light condition refers to LED illumination at 532 nm with 0.175 mW cm^{-2} for PCDTBT:PCBM70 OPD and 770 nm with 0.05 mW cm^{-2} for P3HT:OIDTBR OPD. b) Frequency responses of the OPDs. Dotted line represents the 3 dB cutoff. c) EQE spectra of the OPDs with no bias. EQE spectra of the green, red, and NIR sensors are also using green, red, and gray solid lines, respectively. d) The linear dynamic response of the sensors under green, red, and NIR LED light. The emission spectra of LEDs used are shown in Figure S2 in the Supporting Information.

all of the visible spectra and partially absorbs NIR, with a cut-off wavelength at around 800 nm. The NIR filter (Kodak 89b, Optical Wratten Filter) does not transmit in the visible region and starts transmitting from 700 nm. Combining the two provides the NIR sensor sensitivity from 700 to 800 nm.

2.2. Characterization of Spectral Selective Organic Photodiodes

For PPG and oximetry measurements, ensuring an adequate optical and electrical performance of the OPDs is crucial. **Figure 3**a–c shows optical and electrical characteristics of OPDs fabricated with PCDTBT:PCBM70 or P3HT:O-IDTBR. The OPDs must meet the following two conditions in order to pick up the PPG signal. They must be sensitive enough to detect low light intensities which go through the finger and they must possess adequate frequency response in order to properly detect pulsatile changes in the blood volume. In Figure 3a, both OPDs exhibit high reverse bias dark leakage current, which increases with larger bias. This stems from relatively thin thickness of the photoactive layer. The dark current is minimum at 0 V, which is the short circuit condition. Photocurrents under light conditions are also shown. The photocurrent is steady at the short circuit condition. The frequency responses of each OPD are shown in Figure 3b. The 3 dB frequencies are above 30 kHz for both OPDs, which is much higher than

1 kHz that is required for pulse oximetry. The shapes of the EQE spectra in Figure 3c are similar to the photoactive layer absorption characteristics shown in Figure 2. The sensitivity of PCDTBT:PCBM70 and P3HT:O-IDTBR based OPDs extends to 700 and 800 nm, respectively. The EQE of the green, red, and NIR sensors are also shown. As described in Figure 2, green and red sensors are assembled by covering the light incident side of the PCDTBT:PCBM70 based OPDs with either the green or the red filters, while the NIR sensor is assembled by covering the P3HT:O-IDTBR based OPD with the NIR filter. The resulting green, red, and NIR sensors are spectrally selective having sensitivity peaks at 525, 610, and 740 nm, respectively, with minimal spectral overlap. The linear dynamic responses of each sensors are shown in Figure 3d. The spectra of the LEDs used in this analysis are shown in Figure S2 in the Supporting Information. The photocurrents show linear trend according to the light intensity for all light types. The reliability of the sensors used is also crucial in obtaining meaningful readings. In Figure S3 in the Supporting Information, we tracked the EQE degradation of both PCDTBT:PCBM70 and P3HT:O-IDTBR after PPG measurement. While sensors based on PCDTBT:PCBM70 recorded over 50% of the initial peak EQE for over 20 d, those based on P3HT:O-IDTBR degraded below 50% after 3 d. In order to get the best readings, for vital measurement with sensors based on P3HT:O-IDTBR, we used fresh devices within 2 d of fabrication. Overall, through the characterization, we confirm that
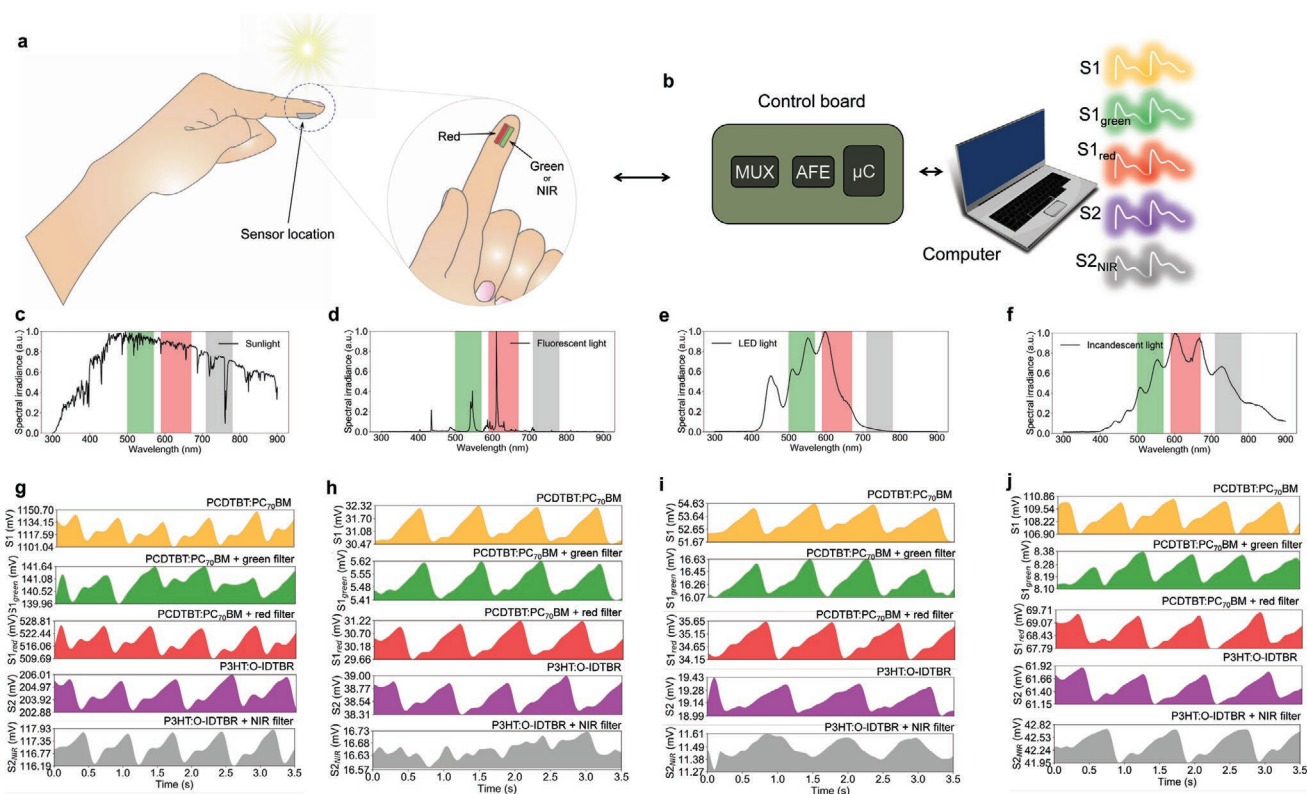
**ADVANCED
SCIENCE NEWS**

www.advancedsciencenews.com

**ADVANCED
MATERIALS
TECHNOLOGIES**

www.advmattechnol.de

Figure 4. PPG measurements under various ambient light conditions using each sensor. a) Schematic illustration of the system setup for acquiring the PPG signal. b) PPG signal processing and transmission. The sensor data are relayed to a multiplexer that switches between the sensors, which is then processed by an analog front end and a microcontroller. Finally, the signal is visualized on a computer. Five sensors are used in the study: PCDTBT:PCBM70 without filter (S1), PCDTBT:PCBM70 with green filter (S1green), PCDTBT:PCBM70 with red filter (S1red), P3HT:O-IDTBR without filter (S2), and P3HT:O-IDTBR with NIR filter (S2NIR). c–f) Normalized light spectrum of sunlight, fluorescent, incandescent, and LED lights, respectively. Sensitivity regions of the green, red, and NIR sensors are shown with shaded areas. g–j) PPG signals obtained under sunlight, fluorescent, incandescent, and LED lights, respectively.

the OPDs have the required sensitivity, selectivity, frequency response, and reliability to resolve PPG signals.

2.3. PPG Measurements for the Ambient Light Oximeter

Pulse oximeters use PPG signals at two different wavelengths to create a ratiometric measurement. This ratiometric measurement is then converted to an oxygenation value.[4] To verify the capability of pulse oximetry using our green, red, and NIR sensors, we recorded PPG signals using our sensors from various ambient light sources. A volunteer puts the sensor on the index finger under a light source as illustrated in **Figure 4**a. The sensor is connected to a multiplexer (MUX) that switches between the red and the green or NIR sensor. The signal is then relayed to an analog front end (AFE), which is controlled by a microcontroller (μC). The PPG current signal is amplified and converted to a voltage signal by the AFE and sent to a computer for processing and visualization (Figure 4b). The light sources we tested include sunlight, fluorescent, incandescent, and LED lights. The spectral irradiance of the light sources is shown in Figure 4c–f. The shaded areas in Figure 4c–f are shown to aid visualization of the sensitivity regions of the green, red, and NIR sensors. Additionally, we labeled five

different combinations of the photoactive layers and filters—PCDTBT:PCBM70 without filter (S1), PCDTBT:PCBM70 with green filter (S1green), PCDTBT:PCBM70 with red filter (S1red), P3HT:O-IDTBR without filter (S2), and P3HT:O-IDTBR with NIR filter (S2NIR). Figure 4g–j shows the PPG signals collected from the four light sources using our five different sensors.

The sun has an abundant amount of green, red, and NIR irradiance (Figure 4c). The PPG signals taken outdoors under sunlight using the sensors S1, S1green, S1red, S2, and S2NIR are shown sequentially in Figure 4g. All of the sensors provide clean PPG signals, which means that both red + green and red + NIR sensor combinations can be used to perform pulse oximetry under sunlight. Fluorescent light measurements are taken indoors where the room is lit by fluorescent lamps, and the distance between the measurement position and the light source is ≈2 m. The spectrum of the fluorescent room light is shown in Figure 4d. The light spectrum has two sharp peaks at 546 and 611 nm. The 546 nm peak is in the green region and 611 nm is in the red region. There is no visible contribution in the NIR region. This is reflected in the PPG measurements in Figure 4h. Distinct PPG signals are observed using S1, S1green, S1red, and S2 sensors, but not with the S2NIR sensor. A desk lamp is used to conduct LED and incandescent light measurements. The distance between the measurement position and the
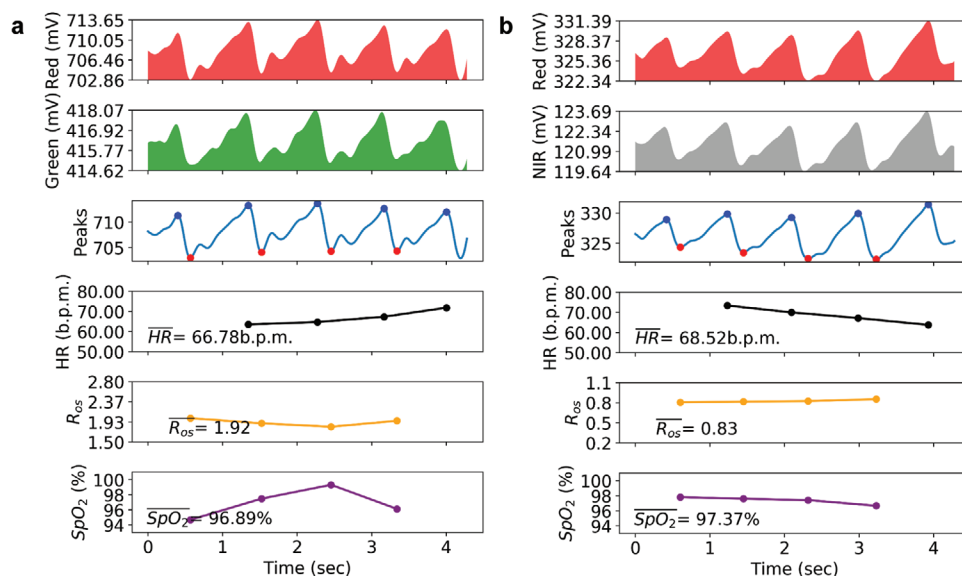
**ADVANCED
SCIENCE NEWS**

www.advancedsciencenews.com

**ADVANCED
MATERIALS
TECHNOLOGIES**

www.advmattechnol.de

Figure 5. Pulse oximetry using the Sun as a light source. Two sensor combinations are used—a) red and green and b) red and NIR. PPG data are collected from the index finger of a volunteer. In both (a) and (b), the top two panels show PPG signals from the sensors, i.e., red and green in (a) and red and NIR in (b). Third and fourth panels from the top show the peaks and heart rate calculated by timing the diastolic peaks. The fifth panel shows the ratio of the ratios of PPG signals (R_{os}), which is used to calculated oxygenation. The bottom panel shows the SpO_2 calculated from R_{os}. The measurement in (a) and (b) are taken at different times.

light source is 20 cm. Figure 4e shows the spectrum of the LED bulb light (Torchstar A19, 5000K). The spectrum includes green and red spectrum, with a very small contribution in the NIR region, which is again confirmed by the PPG measurements in Figure 4i. The signals from S1, S1green, S1red, and S2 are clear. The S2NIR signal is weak and the waveform is not clear. The spectrum of the incandescent light is shown in Figure 4f. It includes all green, red, and NIR regions. Consequently, all of the sensors provide clear PPG signals in Figure 4j.

Since all four light sources provided PPG signals, pulse oximetry measurements using these ambient light sources are possible. The irradiance of the indoor light sources used for the measurements are 0.35, 8.3, and 3.7 mW cm^{-2}, respectively, for fluorescent, incandescent, and LED light. The signal magnitudes of the PPG signals obtained from the four different light sources using the five different OPD and filter combinations are compared in Figure S4 in the Supporting Information. Evidently, the PPG signals obtained from the sunlight demonstrate the highest signal magnitudes. On the other hand, under indoor lighting conditions, the fluorescent lamp provided the lowest signal magnitude. The PPG signals recorded from the incandescent and LED are similar in magnitude. We minimized the measurement variability by accurately placing the sensor for each measurement ensuring a good contact to the skin. Surprisingly, however, the PPG signal magnitudes did not scale linearly with the irradiance of the incident light. A systematic study is needed to find the relationship of signal magnitude variation with the irradiance of the incident indoor lights, which is out of the scope of this paper. Since pulse oximetry is a ratiometric measurement, i.e., PPG signals from two sensors are used—any variation in the source light will be observed on both the sensors. Therefore the variation in incident light will be inherently calibrated. In this work, we

experimentally confirm that pulse oximetry can be performed with the four ambient light sources, although magnitudes of signals may vary.

2.4. Pulse Oximetry Using the Sun as a Light Source

Since the Sun is a broadband light source and provides the best PPG signal magnitudes compared to the other ambient light sources, we opted to perform pulse oximetry outdoors. As discussed previously, the combinations of red and green or red and NIR light can be used to perform pulse oximetry. Sunlight has emission at all the wavelengths required for oximetry. Therefore, utilizing the PPG signal acquisition system shown in Figure 4a,b, we collected PPG signals with the combination of red and green sensors (**Figure 5**a) and red and NIR sensors (Figure 5b). The PPG signals are collected from the index finger of a volunteer. The PPG signals collected from the two sensors are shown in the top two panels of Figure 5a,b. Signals from all the sensors exhibit clear PPG waveforms. The combination of red and NIR provides a signal with low drift, hence, is more reliable. Heartbeat peaks and valleys are detected from the PPG signals—from which heart rate is calculated by timing the peaks. We calculated pulse oxygenation of 96.89% for the red and green combination and 97.37% for the red and NIR combination, respectively.

2.5. Simultaneous Oxygenation Measurements Using the Ambient Light Oximeter and a Commercial Oximeter

In order to validate the ALO, we simultaneously recorded SpO_2 signals from a volunteer using a commercial finger clip sensor and the ALO (red and NIR combination) as shown
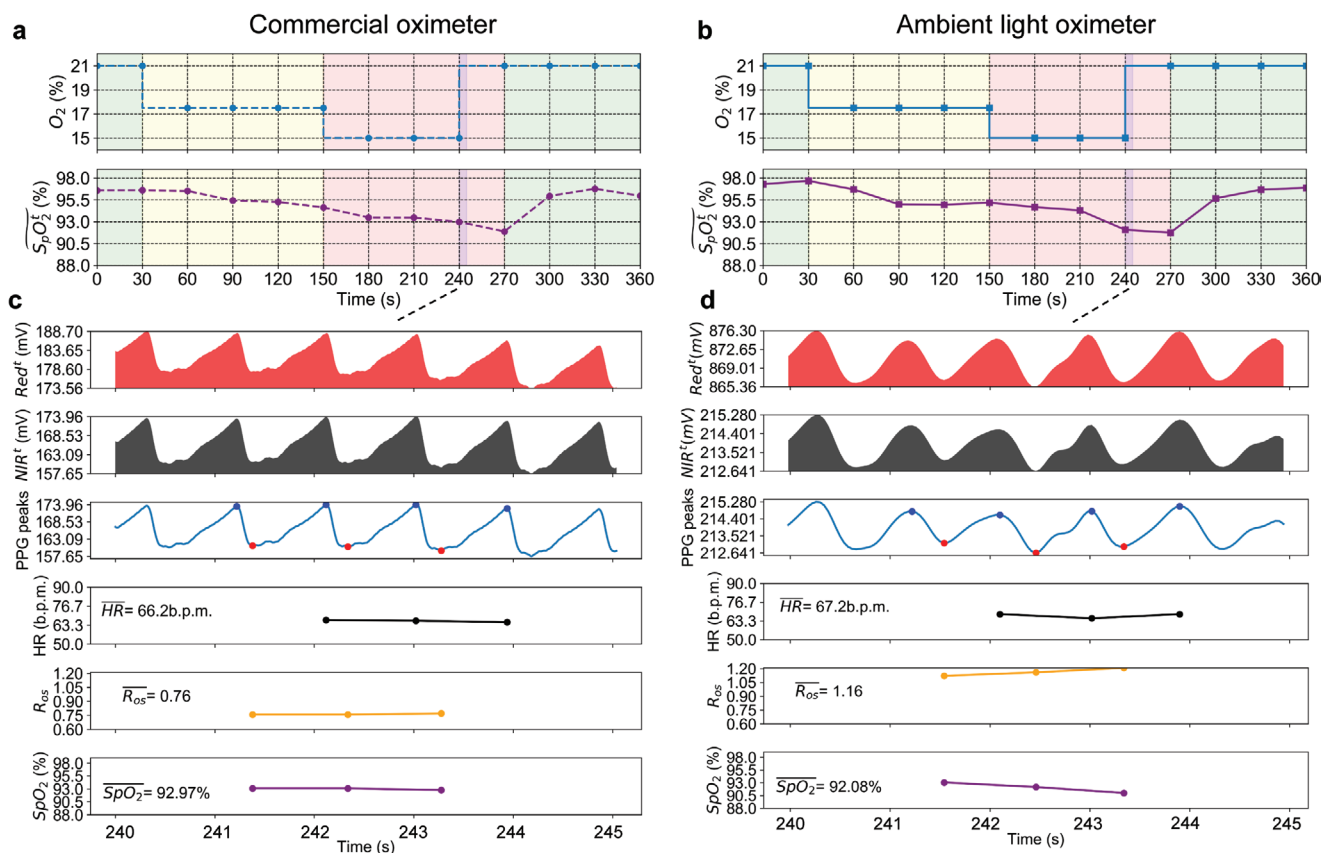
Figure 6. Simultaneous recording of oxygenation using a commercial oximeter and our ambient light oximeter. Pulse oxygenation data are collected from the index finger of a volunteer using a solar simulator as the light source. An altitude simulator is used to change the concentration of inhaled oxygen (O_2%). a,b) Change in O_2% and measured SpO_2 using the commercial oximeter and our ALO, respectively. c,d) Red and NIR PPG signals, signal peaks, calculated heart rate, the ratio of the ratios of the PPG signals, and calculated SpO_2 using the commercial oximeter and our ALO, respectively. The recording is collected from 240 s < t < 245 s.

in **Figure 6**. We used a solar simulator, spectrum which is calibrated to air mass (AM) 1.5G, to perform a controlled experiment. To verify that our oximeter can readily detect changes in oxygen saturation of the body, we used an altitude simulator to change the oxygen content of the air the volunteer breathes in. This change in oxygenation is then recorded using a commercial finger clip sensor (Figure 6a,c) and our ALO (Figure 6b,d). The test setup is described in detail by Khan et al.[4] We varied the concentration of the inhaled oxygen from 21% at t = 0 s to 17.5% at t = 30 s (top panel of Figure 6a,b). After holding at the same oxygen concentration for 2 min, we further reduced the oxygen concentration to 15% and fixed at that level for 2 min before returning to the baseline oxygen concentration of 21%. The recorded SpO_2 from the commercial and the ALO are shown in the bottom panels of Figure 6a,c, respectively. The oximeters start at 96% and 97% baseline SpO_2, for the commercial and the ALO, respectively, and go down to 92% before returning to the baseline values.

The PPG signals collected at 240 s < t < 245 s are shown in Figure 6c,d. The top two panels show the PPG signals, while the third and fourth panels show the PPG signal peaks and calculated heart rate. The fifth and sixth panels show R_{os} and SpO_2. The data for the ALO were collected at 100 Hz,

hence, the dicrotic notch was not resolved in the PPG signals. However, only peak-to-peak amplitudes are required to calculate SpO_2, therefore, we calculated R_{os} values using the peak-to-peak signal magnitudes. We observe an error <1% in SpO_2 for the ALO compared to the commercial oximeter, which is within the 1% to 2% error margin inherent to pulse oximetry.

3. Conclusion

Our oximeter design uses spectrally selective OPDs with light filters. This approach reduces system and mechanical complexity by eliminating the need for a controlled light source, i.e., LEDs. In addition, the sensor design without LEDs eliminates the need for power required to drive the LEDs. Moreover, we employ printing techniques to fabricate the OPDs. The sensors used in our system are compatible with low-cost large-area production. Additionally, the sensors are soft and flexible. Therefore, our ambient light oximeter can make healthcare products more conformable and affordable. Overall, the pulse oximeter with no controlled LEDs is a new concept which can simplify the design of future pulse oximeters, making the overall system low-cost, efficient, light, and comfortable.

The four ambient light sources—sunlight, fluorescent, LED, and incandescent lights provided adequate PPG signal magnitudes for performing pulse oximetry. However, the Sun proved to be the best light source that rendered the highest PPG signal magnitudes. We used two combinations of spectrally selective OPDs to assemble the ambient light oximeter, using red and green or NIR sensors. While all the light sources had visible light spectra, only sunlight and incandescent lights had NIR contributions. Hence, the visible sensor combination, i.e., red and green can be used for all four ambient light sources, and the red and NIR combination can be used for sunlight and incandescent lights. Overall, in this work, we demonstrated pulse oximetry with ambient light sources. We showed that oximetry can be performed only using the sunlight, and with additional improvement, indoor light sources can also be used for pulse oximetry. Our organic optoelectronic sensors equipped with filters show selective responses to green, red, and NIR light, which were used for oximetry. We hope that our demonstration of the ALO will encourage further research on improving OPD performance in both visible and NIR spectrum, developing low-noise signal processing and motion artifact reduction circuitry, and new directions in ambient light oximetry.

Further study and improvement are needed for large-scale implementation of the ALO. One of the limitations of this setup is the OPDs need to face the light sources to get a measurement. Therefore, the current setup by itself will have restricted usage compared to conventional pulse oximetry and will most likely be suitable as a supportive or alternative device that operates in low-power scenarios. Moreover, pulse oximeters, in general, are quite susceptible to motion artifacts. The ALO described here is no different. We did observe motion artifacts in our collected data. Under the sunlight, the signal is stronger than the indoor lighting conditions, therefore, motion artifacts can be accounted for by tracking the baseline signal drift. This phenomenon becomes more challenging under indoor lighting conditions, where the signal strength is weak. Overall, in order to widen the ALO's usage, improvement in the OPD performance and signal processing circuitry, and study on how much light is needed under each condition are required.

4. Experimental Section

Sensor Fabrication: OPDs were printed on top of planarized polyethylene naphthalate (PEN) substrates (DuPont) using a blade coating technique previously reported by Pierre et al.[22] A layer of high conductivity poly(3,4-ethylenedioxythiophene) polystyrene sulfonate (PEDOT:PSS, Sigma-Aldrich 739316-25G) was printed by blade coating (200 µm blade height at 1.6 cm s^{-1}) the solution over prepatterned hydrophilic rectangles in the substrate defined by a 10 s plasma treatment through a stencil. The layer was annealed at 120 °C for 10 min. The photoactive solutions comprised of 1:3 weight ratio of PCDTBT:PCBM70 (Solaris Chem) dissolved to 35 mg mL^{-1} in chlorobenzene or 1:1 weight ratio of P3HT:OIDTBR dissolved to 26 mg mL^{-1} in chlorobenzene were blade coated (2000 µm blade height at 1.6 cm s^{-1}) in a glove box with the substrate heated to 45 °C. Both photoactive layers were annealed at 120 °C for 30 min. The aluminum cathode (100 nm) was thermally evaporated under vacuum at 2×10^{-6} Torr.

Sensor Characterization: Current–voltage characteristics were measured using an Agilent B1500a semiconductor device parameter analyzer inside a shielded probe station. EQEs were measured with

a PV Measurements QEXL system. An Electro Optical Components DHPCA-100 trans-impedance amplifier, Analog Discovery 100MSPS Universal Serial Bus (USB) Oscilloscope, and a Pulse Function Arbitrary Generator (Agilent Technologies, 81150A) were used for frequency measurement. Hamamatsu S2387-66R silicon photodiode and the Agilent B1500a were used to measure light readings from green, red, and NIR LEDs. Spectra of the light sources were measured with a Compact Spectrometer (Thorlabs, CCS200). A Solar Simulator (Newport, 94021A) was used to simulate the illumination under sunlight.

Ambient Light Oximeter System: The ambient light oximeter requires two OPDs connected to the readout electronics. A multiplexer (Analog Devices ADG1608) was used to switch between the two spectrally selective OPDs. A Texas Instruments AFE (AFE4490) was used to sequentially read out the OPD signals at 100 Hz. The AFE was controlled with an Arduino Due microcontroller. A two-stage OPD gain circuitry was used to amplify the photocurrent. Finally, the data were collected using a USB interface and were processed using custom in-house software. All oximetry experiments performed on human subjects were carried out with informed consent under the approval of the University of California, Berkeley Institutional Review Board, protocol ID 2014-03-6081.

Supporting Information

Supporting Information is available from the Wiley Online Library or from the author.

Conflict of Interest

The authors declare no conflict of interest.

[1] A. Challoner, C. Ramsay, *Phys. Med. Biol.* **1974**, *19*, 317.

[2] J. Allen, *Physiol. Meas.* **2007**, *28*, R1.

[3] C. M. Alexander, L. E. Teller, J. B. Gross, *Anesth. Analg.* **1989**, *68*, 368.

[4] Y. Khan, D. Han, A. Pierre, J. Ting, X. Wang, C. M. Lochner, G. Bovo, N. Yaacobi-Gross, C. Newsome, R. Wilson, A. C. Arias, *Proc. Natl. Acad. Sci. USA* **2018**, *115*, E11015.

[5] Y. Khan, D. Han, J. Ting, M. Ahmed, R. Nagisetty, A. C. Arias, *IEEE Access* **2019**, *7*, 128114.

[6] C. M. Lochner, Y. Khan, A. Pierre, A. C. Arias, *Nat. Commun.* **2014**, *5*, 5745.

[7] T. Yokota, P. Zalar, M. Kaltenbrunner, H. Jinno, N. Matsuhisa, H. Kitanosako, Y. Tachibana, W. Yukita, M. Koizumi, T. Someya, *Sci. Adv.* **2016**, *2*, e1501856.

[8] D. Han, Y. Khan, J. Ting, S. M. King, N. Yaacobi-Gross, M. J. Humphries, C. J. Newsome, A. C. Arias, *Adv. Mater.* **2017**, *29*, 1700244.

[9] J. Kim, P. Gutruf, A. M. Chiarelli, S. Y. Heo, K. Cho, Z. Xie, A. Banks, S. Han, K.-I. Jang, J. W. Lee, K.-T. Lee, X. Feng, Y. Huang, M. Fabiani, G. Gratton, U. Paik, J. A. Rogers, *Adv. Funct. Mater.* **2017**, *27*, 1604373.

[10] S. Rhee, B.-H. Yang, H. H. Asada, *IEEE Trans. Biomed. Eng.* **2001**, *48*, 795.

[11] P. K. Baheti, H. Garudadri, *Sixth Int. Workshop IEEE*, IEEE, Berkeley **2009**, p. 144–148.

[12] A. K. Bansal, S. Hou, O. Kulyk, E. M. Bowman, I. D. Samuel, *Adv. Mater.* **2015**, *27*, 7638.

[13] H. Lee, E. Kim, Y. Lee, H. Kim, J. Lee, M. Kim, H.-J. Yoo, S. Yoo, *Sci. Adv.* **2018**, *4*, eaas9530.

[14] H. Zhang, P. Gutruf, K. Meacham, M. C. Montana, X. Zhao, A. M. Chiarelli, A. Vazquez-Guardado, A. Norris, L. Lu, Q. Guo, C. Xu, Y. Wu, H. Zhao, X. Ning, W. Bai, I. Kandela, C. R. Haney, D. Chanda, R. W. Gereau IV, J. A. Rogers, *Sci. Adv.* **2019**, *5*, eaaw0873.

[15] J. A. Rogers, T. Someya, Y. Huang, *Science* **2010**, *327*, 1603.

[16] M. L. Hammock, A. Chortos, B. C.-K. Tee, J. B.-H. Tok, Z. Bao, *Adv. Mater.* **2013**, *25*, 5997.

[17] Y. Khan, A. E. Ostfeld, C. M. Lochner, A. Pierre, A. C. Arias, *Adv. Mater.* **2016**, *28*, 4373.

[18] Y. Khan, A. Thielens, S. Muin, J. Ting, C. Baumbauer, A. C. Arias, *Adv. Mater.* **2019**, 1905279.

[19] T. R. Ray, J. Choi, A. J. Bandodkar, S. Krishnan, P. Gutruf, L. Tian, R. Ghaffari, J. A. Rogers, *Chem. Rev.* **2019**, *119*, 5461.

[20] K. Xu, Y. Lu, K. Takei, *Adv. Mater. Technol.* **2019**, *4*, 1800628.

[21] S. Cai, X. Xu, W. Yang, J. Chen, X. Fang, *Adv. Mater.* **2019**, *31*, 1808138.

[22] A. Pierre, I. Deckman, P. B. Lechene, A. C. Arias, *Adv. Mater.* **2015**, *27*, 6411.

[23] D. Han, H. Kim, S. Lee, M. Seo, S. Yoo, *Opt. Express* **2010**, *18*, A513.

[24] J. Kong, S. Song, M. Yoo, G. Y. Lee, O. Kwon, J. K. Park, H. Back, G. Kim, S. H. Lee, H. Suh, K. Lee, *Nat. Commun.* **2014**, *5*, 5688.

[25] O. Synooka, K.-R. Eberhardt, C. R. Singh, F. Hermann, G. Ecke, B. Ecker, E. von Hauff, G. Gobsch, H. Hoppe, *Adv. Energy Mater.* **2014**, *4*, 1300981.

[26] D. Han, S. Yoo, *Sol. Energy Mater. Sol. Cells* **2014**, *128*, 41.

[27] M. Kielar, O. Dhez, G. Pecastaings, A. Curutchet, L. Hirsch, *Sci. Rep.* **2016**, *6*, 39201.

[28] T. Heumueller, W. R. Mateker, A. Distler, U. F. Fritze, R. Cheachareon, W. H. Nguyen, M. Biele, M Salvador, M. von Delius, H.-J. Egelhaaf, M. D. McGehee, C. J. Brabec, *Energy Environ. Sci.* **2016**, *9*, 247.

[29] D. Han, H. Lee, S. Jeong, J. Lee, J.-Y. Lee, S. Yoo, *Org. Electron.* **2015**, *25*, 31.

[30] S. Holiday, R. S. Ashraf, A. Wadsworth, D. Baran, S. A. Yousaf, C. B. Nielsen, C.-H. Tan, S. D. Dimitrov, Z. Shang, N. Gasparini, M. Alamoudi, F. Laquai, C. J. Brabec, A. Salleo, J. R. Durrant, I. McCulloch, *Nat. Commun.* **2016**, *7*, 11585.

ADVANCED MATERIALS TECHNOLOGIES

Supporting Information

Pulse Oximetry Using Organic Optoelectronics under Ambient Light

Donggeon Han,* Yasser Khan, Jonathan Ting, Juan Zhu, Craig Combe, Andrew Wadsworth, Iain McCulloch, and Ana C. Arias*
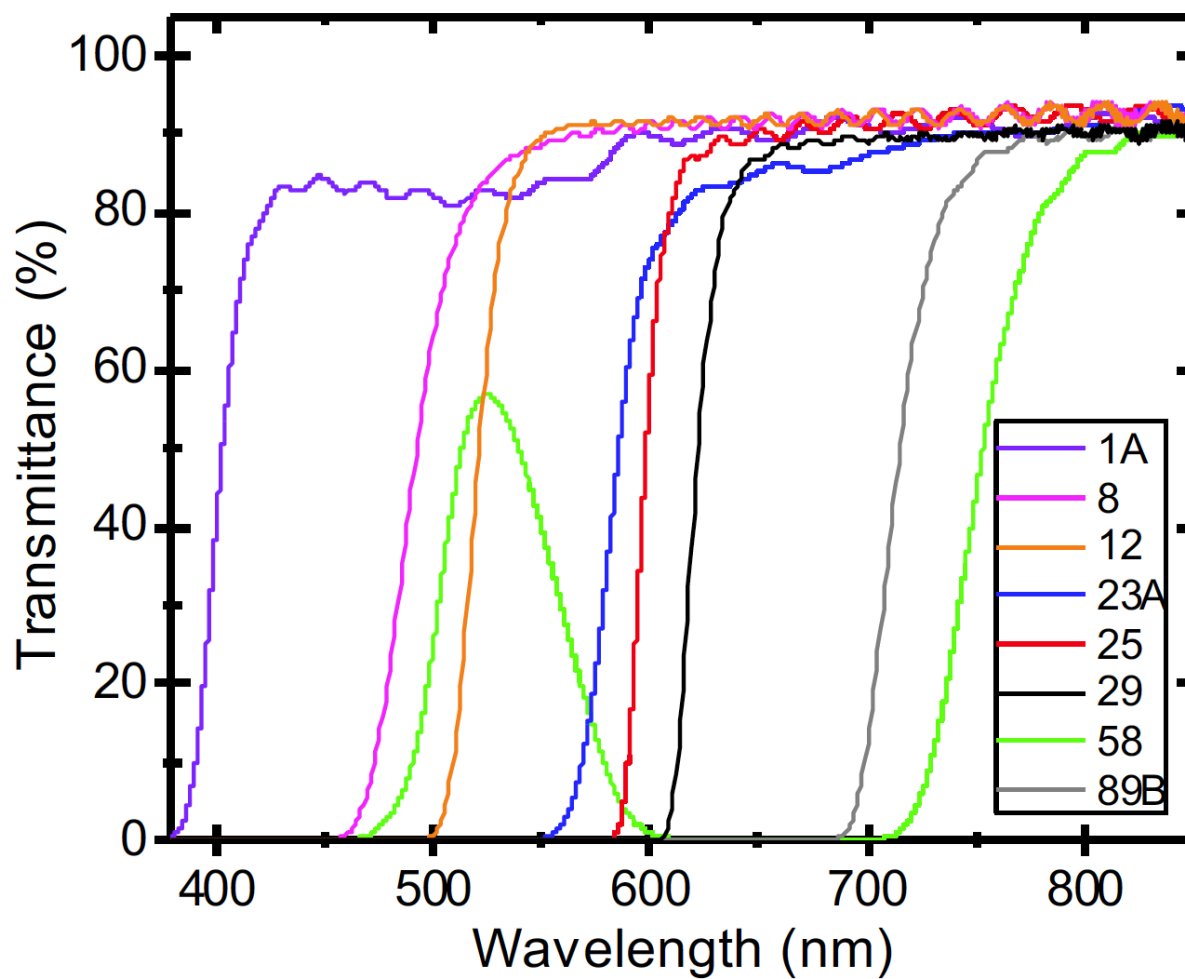
Supporting Information

Pulse oximetry using organic optoelectronics under ambient light

Donggeon Han, Yasser Khan, Jonathan Ting, Juan Zhu, Craig Combe, Andrew Wadsworth, Iain McCulloch and Ana C. Arias

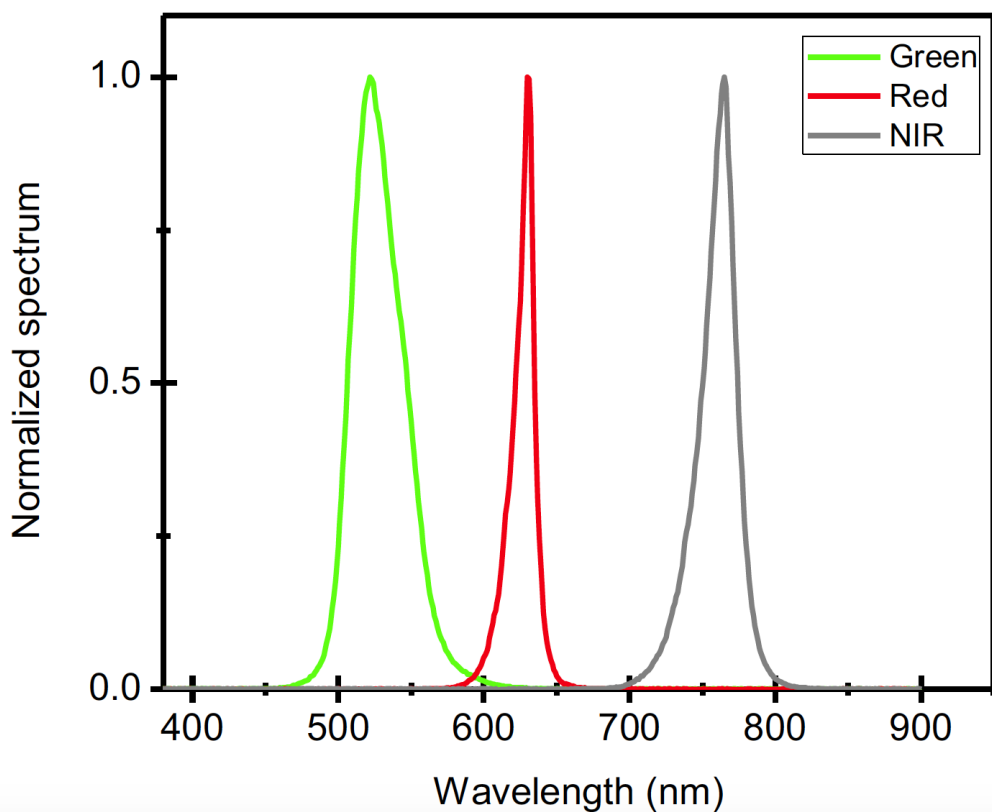**Figure S1.** Transmittance of various filters.

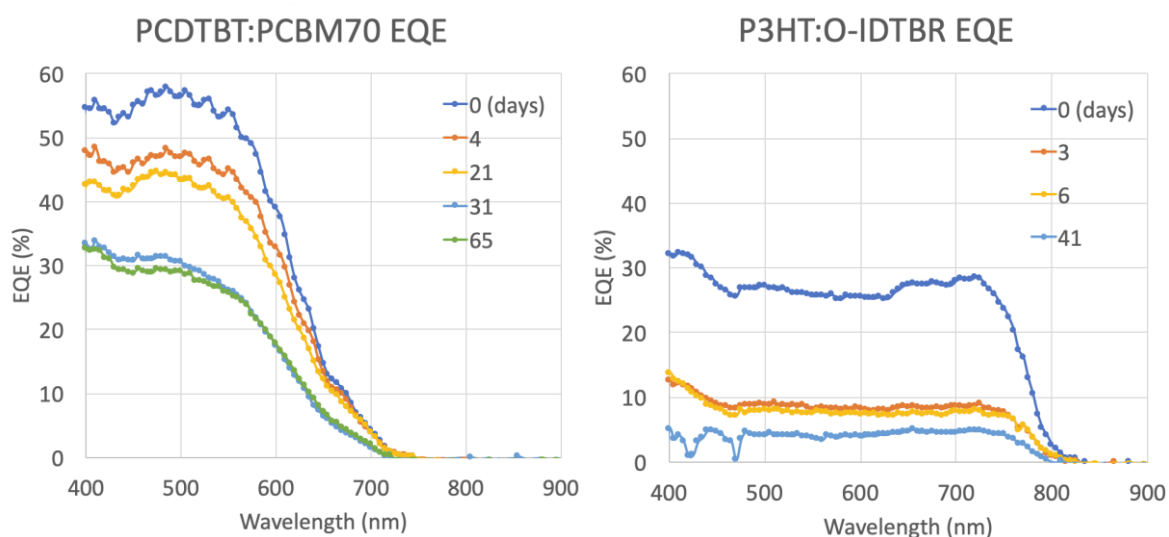**Figure S2.** The spectra of green, red and NIR LEDs used for linear dynamic response measurement in Figure 3d.

Figure S3. Degradation trend of EQE for PCDTBT:PCBM70 (left) and P3HT:O-IDTBR (right).
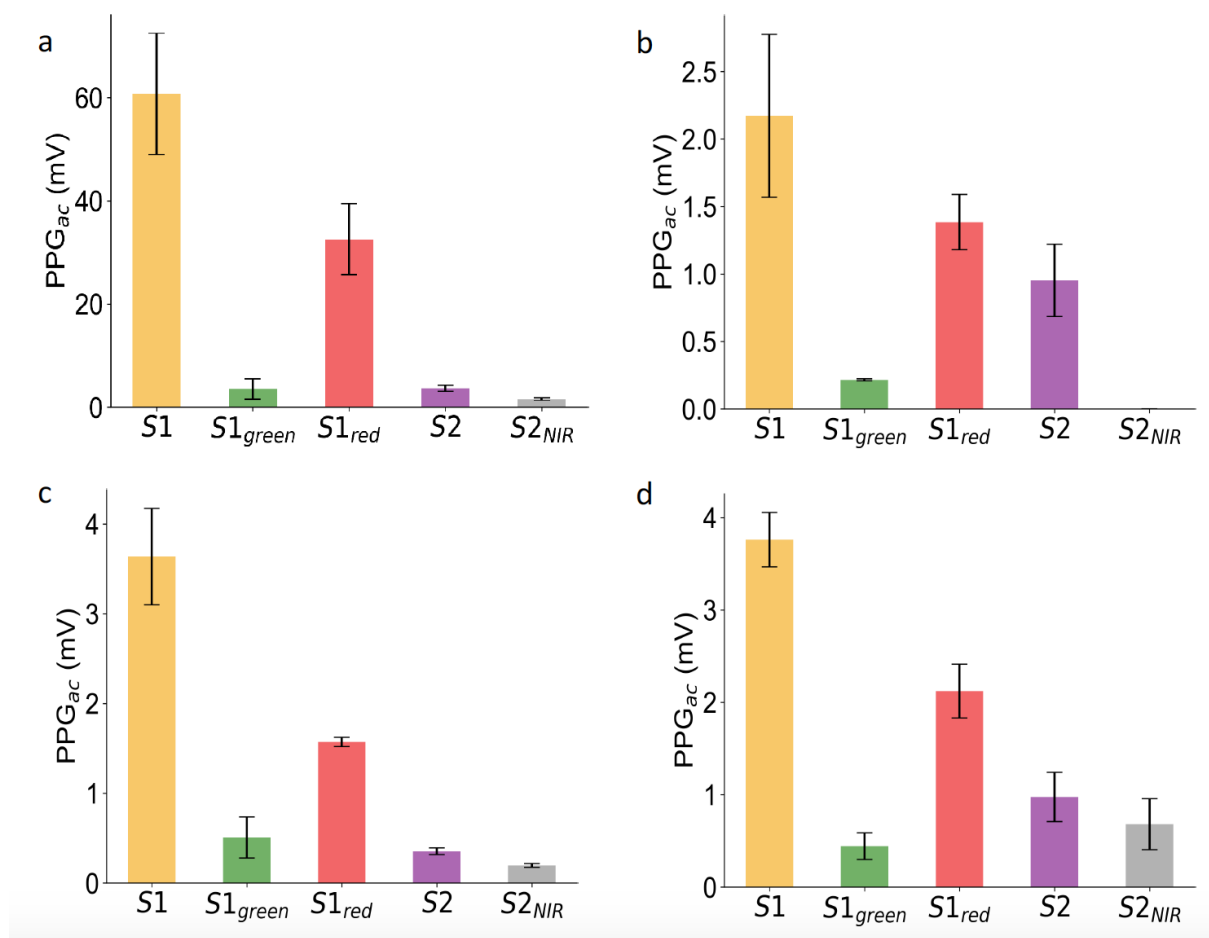
Figure S4. AC signal magnitude of PPG signals collected from the five sensors under the Sun (a), fluorescent lamp (b), white LED lamp (c) and incandescent lamp (d).